Journal of Applied Polymer Science

Development of a Disposable Electrode Modified with Carbonized, Graphene-Loaded Nanofiber for the Detection of Dopamine in Human Serum

Pongpol Ekabutr,[1] Pakakrong Sangsanoh,[1] Poomrat Rattanarat,[2] Charles W. Monroe,[3] Orawon Chailapakul,[2,4] Pitt Supaphol[1,4]

[1]The Petroleum and Petrochemical College, Chulalongkorn University, Bangkok, Thailand

[2]Electrochemistry and Optical Spectroscopy Research Unit, Department of Chemistry, Faculty of Science, Chulalongkorn University, Patumwan, Bangkok 10330, Thailand

[3]Department of Chemical Engineering, University of Michigan, Ann Arbor, Michigan 48109

[4]Center of Excellence on Petrochemical and Materials Technology (PETROMAT), Chulalongkorn University, Patumwan, Bangkok 10330, Thailand

Correspondence to: P. Supaphol (E-mail: pitt.s@chula.ac.th)

ABSTRACT: A one-step electrode surface modification is proposed in which a disposable, screen-printed carbon electrode is functionalized with carbonized, electrospun polyacrylonitrile (PAN)-loaded graphene (G) nanoparticles to form a composite, CPAN5G-4x. The electrochemical behavior of the CPAN5G-4x electrode was examined by cyclic voltammetry and electrochemical impedance spectroscopy. Scanning electron microscopy and X-ray diffraction were used to characterize the surface morphology and physical properties of the carbonized composite nanofibers before and after modification. The modified electrode was found to be effective for the detection of dopamine (DA) using square-wave voltammetry (SWV) in the presence of interfering substances such as ascorbic acid and uric acid. With the addition of sodium dodecyl sulfate (SDS) to an optimized solution of phosphate-buffered saline (PBS) at a pH of 2, the fabricated electrode exhibited enhanced electrocatalytic activity toward the oxidation of DA relative to PBS without SDS at a pH of 7.4. The SWV current displayed a linear response to DA concentrations ranging from 0.5 to 100 μM, with a limit of detection of 70 nM ($S/N = 3$) and a sensitivity of 1.4258 μA μM^{-1} cm^{-2}. Finally, the CPAN5G-4x electrode was used to determine DA levels in human serum. The modified electrode can potentially be harnessed for further electrochemical biosensor applications. © 2014 Wiley Periodicals, Inc. J. Appl. Polym. Sci. **2014**, *131*, 40858.

KEYWORDS: electrochemistry; electrospinning; fibers; graphene and fullerenes; nanoparticles; nanotubes; nanowires and nanocrystals

Received 3 March 2014; accepted 13 April 2014

DOI: 10.1002/app.40858

INTRODUCTION

Dopamine (DA) is an important neurotransmitter that plays a significant role in the mammalian central nervous system, being involved in movement and the mediation of emotions. Abnormal levels of DA have been correlated with Parkinson's disease,[1,2] Alzheimer's disease,[3] and schizophrenia,[4] and can alter the relationship between psychology and the behavior of neurons.[5] Numerous analytical techniques have been used to detect DA, including chromatography,[6] capillary electrophoresis,[7] spectrofluorometry,[8] and surface plasmon resonance.[9] These techniques are time consuming and complicated and require specialized laboratory equipment.[10] Therefore, electrochemical analyses have attracted interest because of their high sensitivity, low cost, rapid detection rate, and effectiveness in diverse biological environments.[11]

The presence of interfering substances poses a principal challenge to the electrochemical detection of DA in complex biological samples. Substances such as ascorbic acid (AA) and uric acid (UA) oxidize at potentials similar to DA, and are typically found in higher concentrations. Various modified electrodes have been studied for the sensitive and selective detection of DA, including a gold electrode modified with poly(3,4-ethylenedioxythiophene),[12] a glassy carbon electrode modified with chitosan,[13] and a microchip electrode with carbon nanotube

Additional Supporting Information may be found in the online version of this article.

(CNT) ink.[14] These electrodes are relatively expensive, however. To lower costs, several researchers have reported alternative sensing approaches based on surface modification of screen-printed carbon electrodes (SPCEs).[10,15–17]

Recent studies have aimed to improve the sensitivity of DA detection by using working SPCEs modified with graphene (G), a flat monolayer of carbon atoms tightly packed into a two-dimensional honeycomb lattice.[18] In comparison to CNTs, G exhibits 60-fold higher conductivity, higher stability, and a higher negative surface charge density, and shows improved DA sensitivity.[19] Carbonized polyacrylonitrile (PAN)-based composite nanofibers are also of interest for electrode fabrication because of their wide variety of applications and straightforward production through electrospinning. After stabilization and carbonization, carbonized nanofibers form a ladder structure via nitrile polymerization[20] that exhibits excellent conductivity and electrochemical activity.[21]

This research aimed to develop a simple method to modify a SPCE using a combination of electrospinning and carbonization of composite nanofibers to enhance electrochemical performance. Sodium dodecyl sulfate (SDS) was also used to further improve DA detection.[22,23] These modifications provide several advantages, including a small sample volume; low cost; high selectivity for DA due to electrostatic interactions with the negatively charged SDS; and promise for large-scale production. The redox responses of unmodified and modified electrodes were evaluated in ferri/ferrocyanide solution using cyclic voltammetry (CV). Square-wave voltammetry (SWV) was used to detect DA with various modified electrodes in phosphate-buffered saline (PBS). Finally, DA content was quantified in the presence of typical interfering molecules (AA and UA), as well as in real human serum.

EXPERIMENTAL

Materials

All materials used in this research were analytical grade. G nanopowder (99.2% C) with an average flake thickness of 12 nm was purchased from Graphene Supermarket. *N*,*N*-dimethylformamide (DMF), dopamine hydrochloride (DA), SDS, hydrochloric acid (HCl), potassium ferricyanide ($K_3[Fe(CN)_6]$), potassium ferrocyanide ($K_4[Fe(CN)_6]$), AA, UA, trichloroacetic acid (TCA), human serum, and polyphosphate-buffered saline (PBS) were purchased from Sigma-Aldrich. PAN with a molecular weight of ~55.5 kDa was used as raw material in the electrospinning process and was obtained from Thai Acrylic Fiber (Thailand). The PBS was adjusted to pH 2 using 1.0*M* HCl. Carbon ink (C2070424D2) purchased from the Gwent Group (Torfaen, UK). Silver chloride ink (Electrodag 7019) was obtained from Acheson Colloids. All chemicals were used as received without further purification. The electrospinning apparatus was a Gamma High Voltage Research Model D-ES30PN/M692 equipped with a DC power source.

The electrochemical measurements were performed using a potentiostat (PGSTAT302N, Metrohm) at room temperature (25 ± 1°C). CV and SWV were performed using a three-electrode system, which consisted of the modified or unmodified SPCE as the working electrode (WE), with a working area of 0.50 cm^2; an Ag/AgCl electrode as the reference electrode; and a carbon plate as the counter electrode.

SPCE Fabrication

SPCEs were produced using 10×25 mm^2 PVC sheets as a substrate. In the first step, silver ink was spread over the PVC surface twice using a manual screen-printing technique, after which the PVC was kept in a drying oven at 60°C for 60 min to evaporate any excess solvent. Second, two carbon layers were coated on the silver layer. Finally, the plastic insulator layer was coated on the top layer. All fabricated SPCEs were stored in a desiccator prior to subsequent surface modification steps.

Preparation of Carbonized Electrospun PAN/G Composite Nanofibers

The 11 wt % PAN solution used for electrospinning was prepared by adding PAN to DMF in a glass vial, followed by vigorous magnetic stirring at 60°C for 6 h. The SDS surfactant was added to obtain a 10 m*M* concentration, and stirred until complete dissolution. Subsequently G powder was added to obtain the final concentrations shown in Table I; after addition of G, solutions were sonicated for 4 h with a homogenizer.

The electrospinning apparatus for producing nanofibers is shown in Figure 1. A 20 mL syringe with a capillary tip ($D = 0.5$ mm) was placed and clamped near an anode connected to a high-voltage power supply. The cathode was connected to an aluminum foil, which was subjected to an applied voltage of 15 kV relative to the anode. The distance between the electrode and nozzle was 15 cm. The collected samples were labeled to indicate the presence of PAN and the percentage of G loading. After electrospinning under ambient conditions, the electrospun samples were stabilized in a muffle oven under air atmosphere at 280°C for 2 h, and then carbonized in a nitrogen atmosphere at a ramp rate of 5°C min^{-1} up to 800°C, where they were held for 3 h. The carbonized nanofibers were ground to a powder and labeled as CPAN followed by the percentage of G loading.

Preparation of Modified Electrodes

Figure 1 presents a schematic illustrating the electrode fabrication process. SPCEs modified with carbonized substances were prepared by casting 5 μL of the carbonized substance at various concentrations (cf. Table I) on the carbon layer of the WEs. After drying in an oven at 60°C for 2 h, the modified electrodes were rinsed with ultra-pure water. Unmodified electrodes were labeled as bare, and the modified electrodes treated with carbonized nanofibers were labeled as CPAN followed by the percentage of G loading. All modified electrodes were stored in a desiccator at room temperature prior to use.[24]

Physical Properties of Carbonized Nanofibers

The surface morphologies of samples before and after carbonization were observed using a Hitachi S-4800 field-emission scanning electron microscope (SEM) operated at 15 kV; SemAphore 4.0 Software was used for image processing. The fiber also observed under transmission electron microscope (TEM). X-ray data were collected using an X-ray diffractometer (Rigaku Smartlab, Japan) based on Cu-Kα radiation. The 2θ angle of the diffractometer was stepped from 5° to 90°.

Table I. Electrochemical Data for Each Modified Electrode

Modification substances	Concentration (mg mL^{-1})	Fiber diameter (nm)		Anodic current densities of various electrochemical methods (μA cm^{-2})				
		Before CBN	After CBN	CV[a] of 1 m*M* $Fe^{3-/4-}$	CV[a] of 40 μ*M* DA	SWV[b] of 40 μ*M* DA	ΔE_p (mV)[a]	I_{pa}/I_{pc}[a]
Bare	-	-	-	20.7 ± 0.5	14.5 ± 0.5	17.2 ± 0.5	872 ± 30	4.2 ± 0.2
CPAN	5	126 ± 16	102 ± 10	26.2 ± 0.6	21.7 ± 0.5	39.1 ± 0.8	769 ± 32	3.1 ± 0.1
CPAN0.5G	5	128 ± 19	116 ± 15	26.5 ± 0.3	25.8 ± 0.4	41.1 ± 0.8	419 ± 40	2.6 ± 0.2
CPAN1G	5	134 ± 20	121 ± 12	29.2 ± 0.8	35.1 ± 0.2	47.3 ± 0.8	204 ± 42	2.0 ± 0.1
CPAN3G	5	145 ± 16	137 ± 17	44.3 ± 0.3	37.9 ± 0.7	55.6 ± 0.4	17 ± 4	1.6 ± 0.1
CPAN5G[c]	5	151 ± 21	144 ± 19	47.8 ± 0.3	44.9 ± 0.2	67.9 ± 0.3	15 ± 4	1.3 ± 0.1
CPAN5G-2x[c]	10	151 ± 21	144 ± 19	57.5 ± 0.6	56.8 ± 0.6	73.3 ± 0.7	15 ± 2	1.2 ± 0.1
CPAN5G-4x[c]	20	151 ± 21	144 ± 19	66.0 ± 0.7	66.8 ± 0.9	81.2 ± 1.1	15 ± 1	1.1 ± 0.2
CPAN5G-6x[c]	30	151 ± 21	144 ± 19	61.4 ± 1.6	63.4 ± 1.5	79.6 ± 1.0	15 ± 5	1.1 ± 0.1

[a] Denotes a CV method with a scan rate of 50 mV s^{-1} in 0.1*M* PBS at a pH of 7.4 ($n = 3$).
[b] Denotes a SWV method in 0.1*M* PBS containing 5 m*M* of SDS at a pH of 2 ($n = 3$). CBN denotes the carbonization process.
[c] Denotes the use of the same CPAN5G to modify the electrode surface.

CV of Modified Electrodes

Electrochemical responses of both modified and unmodified electrodes were characterized using single-loop CV experiments, comprising a forward sweep in the anodic direction from −1 V vs. Ag/AgCl up to 1 V, followed by a sweep back down to −1 V. Voltammograms were measured for 0.1*M* PBS at pH of 7.4 a number of scan rates to establish background currents. To evaluate electrochemistry, the current response of 1 m*M* $[Fe(CN)_6]^{3-/4-}$ and 40 μ*M* DA in 0.1*M* PBS at a pH of 7.4 was evaluated at a number of scan rates, and corrected by subtracting out the corresponding background currents. Redox activity was quantified by measuring anodic and cathodic peak currents (i_{pa} and i_{pc}, respectively) and peak voltages (E_{pa} and E_{pc}) as functions of root scan rate. Peak currents were measured relative to extrapolated baseline currents, according to the graphical procedure illustrated in the Supporting Information. The sample volume was 50 μL for all electrochemical measurements.

Electrochemical Impedance Spectroscopy (EIS)

EIS was conducted using an Autolab potentiostat PGSTAT302N (Metrohm). Impedance spectra for the electrodes were measured in 1 m*M* $[Fe(CN)_6]^{3-/4-}$ in 0.1*M* PBS with a pH of 7.4. The frequency range of the EIS measurement was 0.01–100 kHz, and 100 data points were collected using a 10 mV signal amplitude at a bias potential of +0.4 V vs. Ag/AgCl. All experiments were performed in triplicate.

Square Wave Voltammetry (SWV) of the Modified Electrodes to Detect DA

For the SWV measurements, the optimum parameters were determined in preliminary studies (data not shown) to be a pulse amplitude of 60 mV, a square wave frequency of 18 Hz, and a step height of 5 mV for scanning the potential between −0.3 and 1.6 V vs. Ag/AgCl. This optimized potential control scheme was used in further studies.

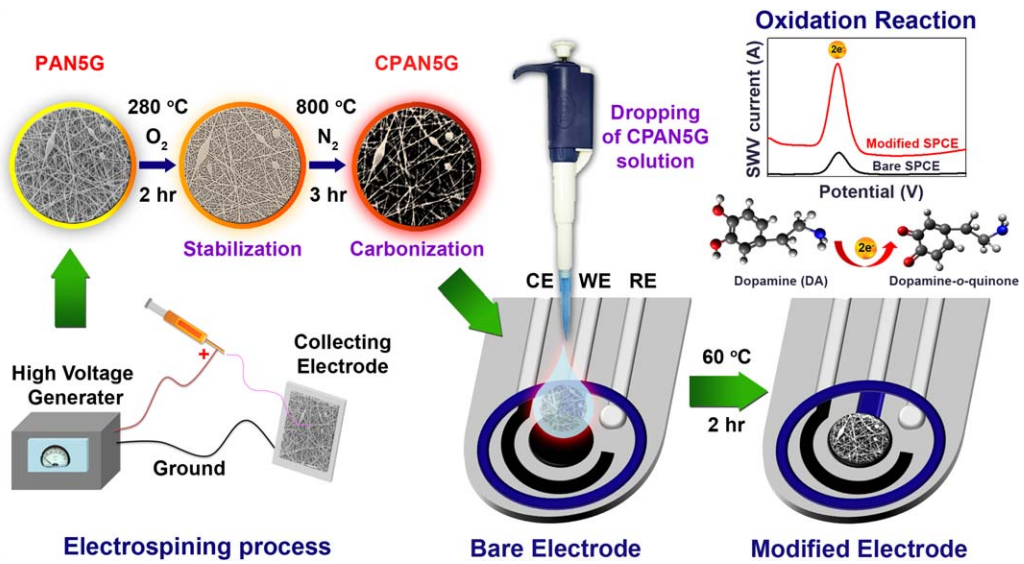

Figure 1. Schematic of SPCE surface modifications. [Color figure can be viewed in the online issue, which is available at wileyonlinelibrary.com.]

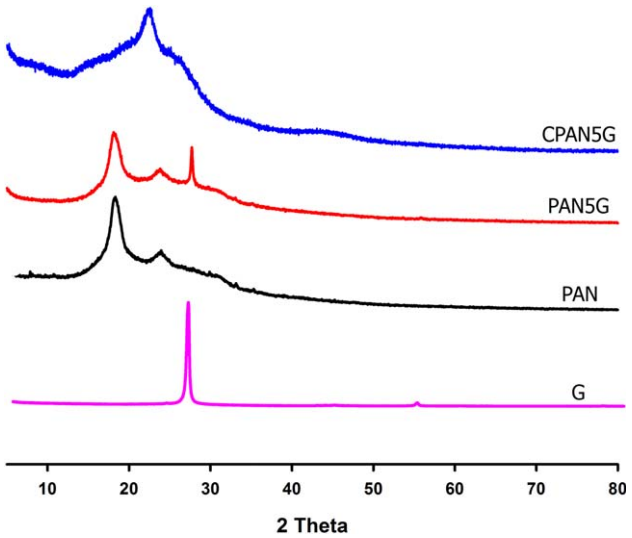

Figure 2. (a) SEM image of PAN5G before carbonization, (b) SEM image of CPAN5G after carbonization and (c) TEM image of CPAN5G after carbonization. [Color figure can be viewed in the online issue, which is available at wileyonlinelibrary.com.]

Analysis of Human Serum

Human serum is a complex biological system but contains no DA. To determine the amount of DA in human serum, known DA concentrations were added to serum using a standard addition method.[10] The protein in the serum was precipitated by the TCA precipitation method,[25] and samples were centrifuged at 15,000 rpm for 10 min. The serum supernatants were retained for further studies.

RESULTS AND DISCUSSION

Preparation and Characteristics of the Electrospun Composite Nanofibers

The G content in the nanofibers was determined to be ~0.5–5 wt % by calculating the net weights of G and PAN in the precursor. To disperse the G particles in PAN solution, 10 m*M* of the anionic surfactant SDS was used. The PAN and PANG composite nanofibers were processed by electrospinning according to previously described methods.[26] Both the morphology and fiber diameter of each sample were evaluated from SEM images. As observed in SEM, nanofibers with G contents of 0–5 wt % were randomly distributed in a 3D nanofibrous web structure. On average, the fiber diameter increased due to the high conductivity of the PAN solution.[27] Bead structures representing partially caused by charge accumulation during electrospining process have also been observed when G content was added.[28] Table I present the average fiber diameters prior to carbonization. Previous electrospinning studies reported that in the presence of SDS in a polymer solution, the fiber diameter (126 nm) increased in comparison to that (266 nm) in solutions lacking SDS,[29] because SDS increases the conductivity of PAN solutions.[27] However, increases in nanofiber diameter can also be observed with high G contents due to increases in the solution viscosity.[30] In this study, we were unable to use G contents greater than 5 wt % for electrospinning because of the prohibitively high viscosity of the polymer solution.

Following stabilization and carbonization at high temperatures (280–800°C), the nanofibers were heated and formed a ladder structure through exothermic reactions, which may include dehydrogenation, cyclization, and crosslinking.[20,31,32] Therefore, the nanofiber diameters for each composition were slightly decreased with partial uniformity, and the fibers were shortened and exhibited low aspect ratios after grinding.[24] The embedded G particles in the carbonized nanofiber can be observed by SEM, as shown in Figure 2(a,b). Moreover, the TEM image in Figure 2(c) confirmed that G particles were well dispersed in carbonized fiber.

Figure 3 displays the X-ray diffraction patterns of PAN, G, PAN5G, and CPAN5G. A diffraction peak typical of G was observed at $\sim 2\theta = 26°$, indicating a (002) plane[33] and thus a hexagonal G structure.[34] In comparing the PAN5G and CPAN5G results, a typical peak from the PAN5G nanofibers could be observed at $2\theta = 17°$.[35,36] Following the carbonization process, the peak sharpness decreased, and a small peak appeared at $2\theta = 22$–$23°$ due to (002) diffraction, indicating the formation of aromatic structures through cyclization.[37] The carbonized samples were stabilized in a muffle furnace under stress, and the CPAN5G exhibited a high proportion of conjugated nitrile groups and higher orientation and larger crystal sizes than PAN5G.

Electrochemical Behavior of Modified Electrodes

The electrochemical behavior of the modified electrodes was recorded by CV using 1 m*M* $[Fe(CN)_6]^{3-/4-}$ as a model redox couple.[38] Table I provides the recorded anodic current data, ΔE_p and I_{pa}/I_{pc}. Figure 4(a,b) present the oxidation potential of each electrode following surface modification by the various carbonized substances. For the carbonized nanofibers containing G, the oxidation potential shifted to lower values and the I_{pa}/I_{pc} values decreased to a value of ~1. Although the CPAN5G-4x (4x indicating four times the smallest concentration of the modified substance used, cf. Table I) exhibited the highest anodic current response with a small peak potential separation ($\Delta E_p = E_{pa} - E_{pc}$) of 15 ± 1 mV, the smaller ΔE_p values revealed the faster electron-transfer kinetics and excellent electrochemical sensitivity of this electrode surface.[16] The use of higher concentrations of modified substance (CPAN5G-6x) resulted in lower anodic current responses than CPAN5G-4x, presumably because thicker films can create a current barrier on the electrode surface.[29]

Figure 5 illustrates the characteristic CV of CPAN5G-4x and bare electrodes in 0.1*M* PBS with a pH of 7.4 at various scan rates (10–600 m Vs^{-1}). Upon increasing the scan rate, the anodic and cathodic current increased linearly, and the oxidation peak and reduction peak potentials shifted slightly.[16] The oxidation peak current, I_{pa}, and reduction peak current, I_{pc}, were assumed to follow the Randle-Sevick relation

$$I_p = kn^{3/2}AD^{1/2}C^b v^{1/2} \quad (1)$$

where the constant k is equal to 2.72×10^5, n is the number of moles of electrons transferred per mole of electroactive species ($[Fe(CN)_6]^{3-/4-}$), A is the electrode area in cm^2, D is the diffusion coefficient in cm^2 s^{-1}, C^b is the bulk solution

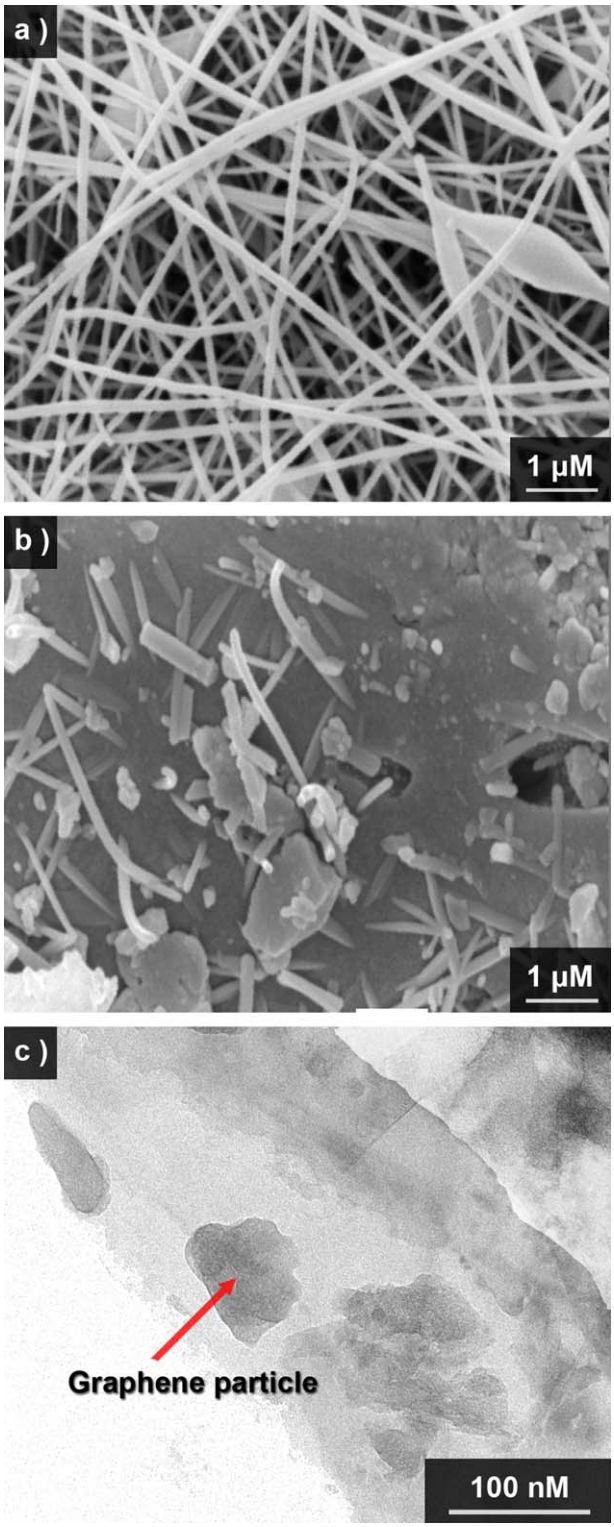

Figure 3. XRD patterns of G, PAN, PAN5G, and CPAN5G nanofibers. [Color figure can be viewed in the online issue, which is available at wileyonlinelibrary.com.]

concentration in mol L^{-1}, and υ is the potential scan rate in Vs^{-1}. Generally the peak current I_p is linearly proportional to the bulk concentration of the electroactive species, C^b, and to the square root of the scan rate, $\upsilon^{1/2}$. The anodic and cathodic peaks exhib-

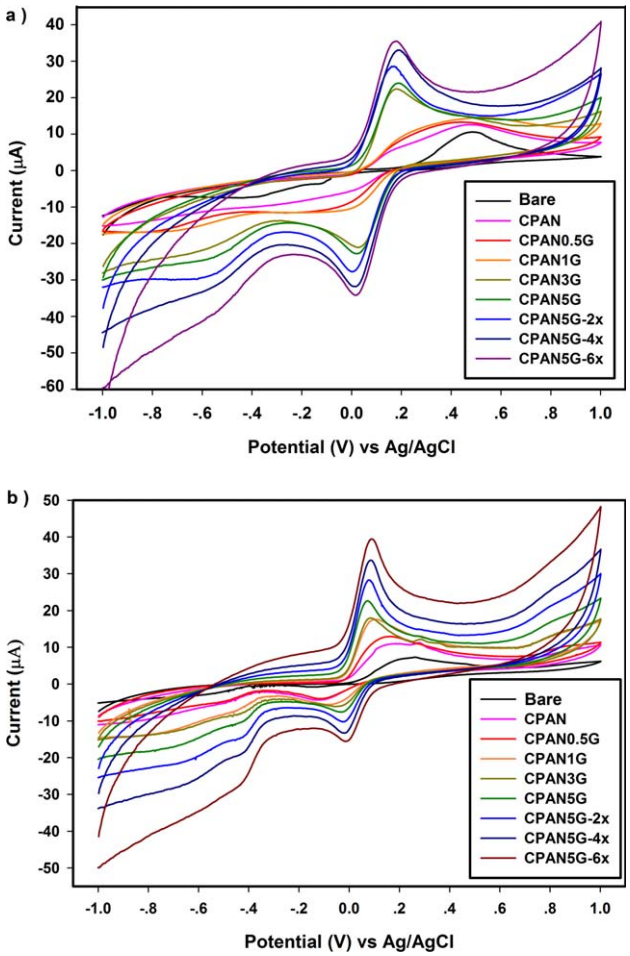

Figure 4. (a) CV images of unmodified/modified electrodes with a scan rate of 50 mV s^{-1} in 0.1*M* PBS at a pH of 7.4, (a) in 1 m*M* $[Fe(CN)_6]^{3-/4-}$ and (b) in 40 μM DA. [Color figure can be viewed in the online issue, which is available at wileyonlinelibrary.com.]

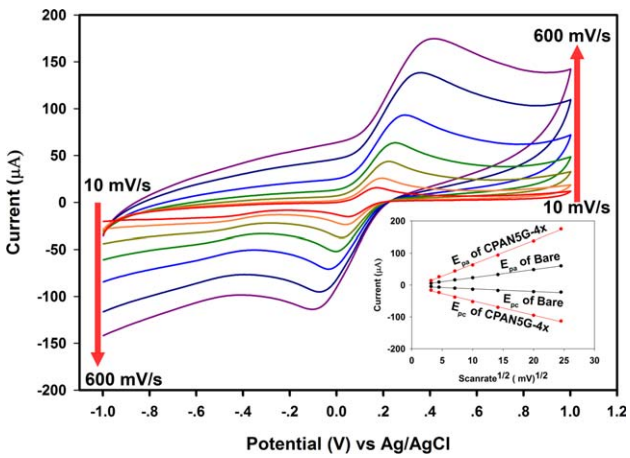

Figure 5. CV images of the CPAN5G-4x electrode measured using 1 m*M* $[Fe(CN)_6]^{3-/4-}$ in 0.1*M* PBS at a pH of 7.4 at different scan rates. Inset is the plot of the linear relationship between the current and scan rate$^{1/2}$ for the bare and CPAN5G-4x electrodes. [Color figure can be viewed in the online issue, which is available at wileyonlinelibrary.com.]

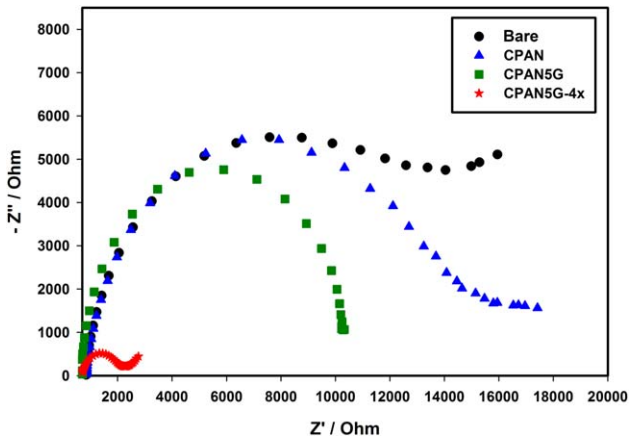

Figure 6. EIS of BARE, CPAN, CPAN5G, and CPAN5G-4x in 1 m*M* $[Fe(CN)_6]^{3-/4-}$ in the presence of 0.1*M* PBS at a pH of 7.4. [Color figure can be viewed in the online issue, which is available at wileyonlinelibrary.com.]

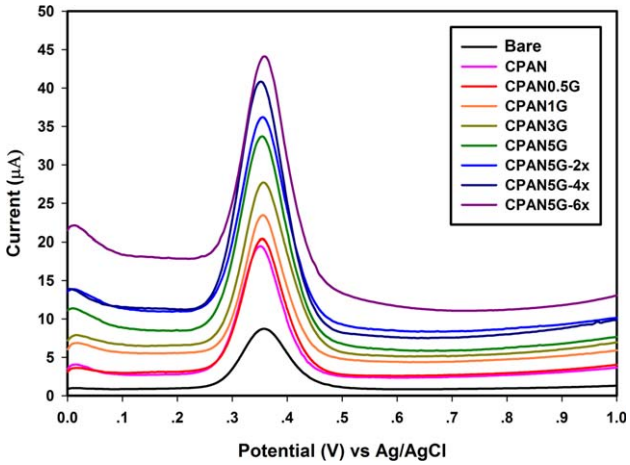

Figure 7. SWV profiles of the unmodified and modified electrodes in 0.1*M* PBS/5 m*M* SDS at a pH of 2. SWV detection conditions: pulse amplitude = 0.06 V, square wave frequency = 18 Hz, and step height = 0.005 V. [Color figure can be viewed in the online issue, which is available at wileyonlinelibrary.com.]

ited nearly equal peak currents. A linear relationship was observed between the peak current and square root of the scan rate, and the inset in Figure 5 provides a comparison of this relationship for $[Fe(CN)_6]^{3-/4-}$ at the bare and CPAN5G-4x electrodes, with the increase in peak spread suggesting a quasi-reversible electrode reaction. Moreover, the incorporation of G particles in the carbonized nanofibers on the screen-printed electrode surface enabled the CPAN5G-4x system to be quasi-reversible ($I_{pa}/I_{pc} = 1$).

EIS was used to investigate the impedance responses of the modified electrode surfaces. Nyquist plots of the impedance spectra show a semicircular region and linear region. The semicircular region gives information about interfacial charge-transfer resistance R_p, whereas the low-frequency Warburg region signifies a diffusion process.[33] R_p can be used to explain the interfacial properties of the electrode.[12] The CPAN5G-4x electrode exhibited the smallest semicircular region in Figure 6, suggesting that a low charge-transfer resistance resulted in the promotion of electro-oxidation and enhanced catalytic activity of the modified electrode.[12,29] This result demonstrates that the CPAN5G-4x produced by this method will be a promising electrode in electrochemical sensor applications.

Determination of DA at Different Modified Electrodes

DA detection was performed using CV to detect 40 μM DA at each electrode in 0.1*M* PBS with a pH of 7.4, as shown in Figure 4(b). A pair of peaks was observed at each electrode, corresponding to the redox couple of DA. These experiments confirmed that DA can be detected by CV. The use of CPAN5G-4x to modify the electrode surface resulted in larger anodic currents for DA (66.8 ± 0.9 $\mu A\ cm^{-2}$) at a low oxidation potential (70 mV). These results are supported by the observations of the anodic current of $[Fe(CN)_6]^{3-/4-}$ in section "Electrochemical Behavior of Modified Electrodes."

SWV is a superior method for the detection of DA, offering several advantages, such as excellent sensitivity. Background currents can be eliminated by using the difference between the forward and reverse peak currents ($i_{for} - i_{rev}$) as a gauge of electrochemical activity. The peak height so measured is directly proportional to the DA concentration. In this study, each electrode was evaluated in an optimized solution (0.1*M* PBS containing 5 m*M* SDS with a pH of 2), as shown in Figure 7, which depicts the sharp curves for each electrode at an oxidation potential of ~+0.36 V. The calculated currents are listed in Table I. CPAN5G-4x clearly exhibited the highest peak anodic current for the conversion of DA to dopamine-*o*-quinone,[33] and was therefore selected for use in further studies.

Analysis of Ternary Mixtures of DA, UA, and AA at CPAN5G-4x: Effect of SDS

Figure 8(a) presents typical SWV traces for the individual determination of DA, UA, AA, and mixtures of these compounds at a CPAN5G-4x electrode in 0.1*M* PBS without SDS at a pH of 7.4 (simulated human serum). AA and UA are typically found in human bodily fluids at concentrations 100- to 1000-fold higher than that of DA.[10,39] In human serum, the levels of AA and UA are 80 and 400 μM, respectively[40]; in this study, the concentrations of AA and UA in the supporting electrolyte were therefore maintained at those concentrations. Previous reports have found that SPCEs or glassy carbon electrodes are unable to distinguish mixtures due to overlapping anodic currents.[41] As a result, these electrodes are not suitable for the detection of DA in the presence of AA and UA. In contrast, the CPAN5G-4x electrode was able to distinguish the DA peak (+70 mV) from the UA peak (+280 mV). Interestingly, the oxidation curve for AA did not exhibit an obvious peak in this system. Indeed, previous studies reported that electrodes modified by G, which contains a high density of negative charges, exhibit interference from AA as well.[42] However, the peaks of DA and UA in the mixture were shifted to higher positive potentials of ~+180 and +350 mV, respectively, with a potential difference ($E_{UA} - E_{DA}$) of ~200 mV, presumably because the diffusion of DA molecules to the electrode surface was disturbed by the UA molecules at a pH of 7.4.

In the presence of 5 m*M* SDS at pH 2, as shown in Figure 8(b), CPANG5-4x exhibited increased separation of the oxidation

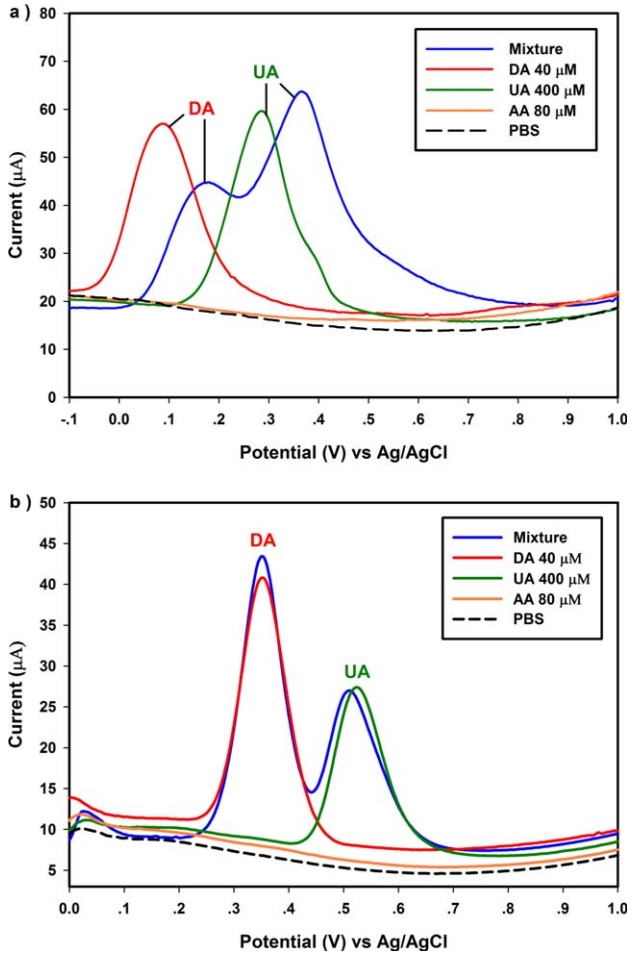

Figure 8. SWV profiles of CPAN5G-4x in the presence of 40 μM DA, 80 μM AA, and 400 μM UA in (a) 0.1M PBS with a pH of 7.4 and (b) 0.1M PBS/5 mM SDS with a pH of 2. [Color figure can be viewed in the online issue, which is available at wileyonlinelibrary.com.]

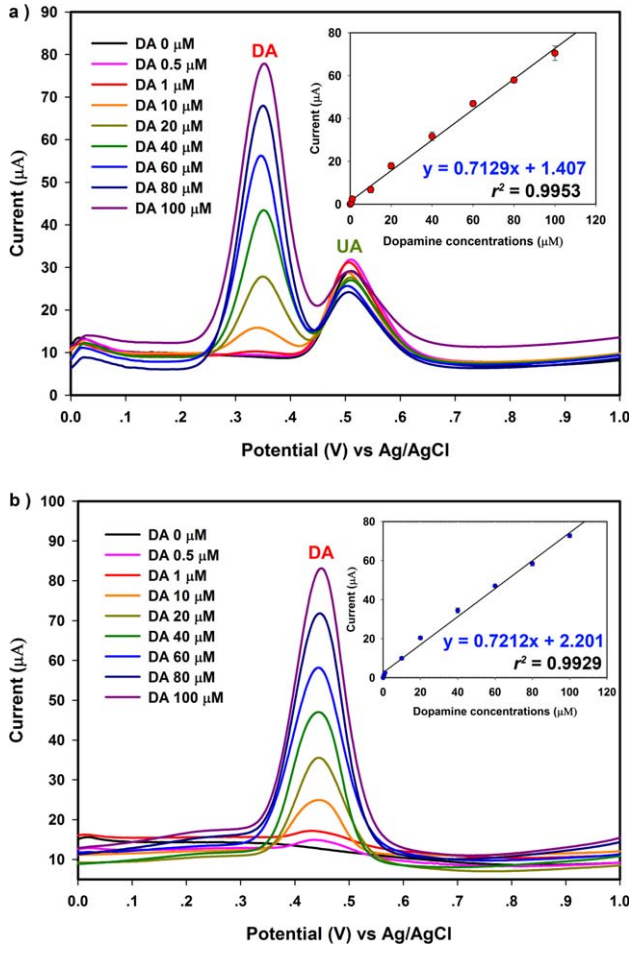

Figure 9. (a) Representative SWV profiles of the CPAN5G-4x electrode in 0.1M PBS/5 mM SDS at a pH of 2; The inset of (a) is the calibration curve for DA detection over a concentration range of 0.5–100 μM in the presence of AA and UA at 80 and 400 μM, respectively; (b) Representative SWV profiles of the CPAN5G-4x electrode in human serum after TCA protein precipitation; The inset of (b) is the calibration for different spiked DA concentrations over the range of 0.5x–100 μM. [Color figure can be viewed in the online issue, which is available at wileyonlinelibrary.com.]

peaks of DA and UA under the same concentrations used in the non-SDS system. SDS is an anionic surfactant that can adsorb on the CPAN5G-4x electrode surface in admicellar and micellar forms, depending on the surfactant concentration. The negatively charged film will orient with the hydrophilic region of the molecules facing the aqueous medium and the hydrophobic tail aligned to the electrode surface. Accordingly, in the optimized solution (pH = 2), a UA ($pK_a = 5.7$) peak is observed at +530 mV and the DA ($pK_a = 8.8$) peak shifts to less positive potential due to electrostatic interaction.[10] In addition, positively charged DA^+ can easily accumulate and diffuse to the hydrophobic region of the aligned SDS molecules, resulting in more rapid electron transfer from DA and a sharp, well-defined anodic peak for DA at +350 mV.[12] As a result, this electrode can selectively detect DA in the presence of high concentrations of UA and AA in the optimized solution.

The calibration curve for DA in the presence of 400 μM UA, 80 μM AA, and 5 mM SDS in optimized PBS solution was determined using SWV, as shown in Figure 9(a). The linear relationship between the DA concentration and oxidation current was described by the equation $I_{DA} = 0.7129C_{DA} + 1.407$ with a correlation coefficient of 0.9953 ($n = 3$) in the range of 0.5–100 μM. The LOD and sensitivity were calculated to be 70 nM ($S/N = 3$) and 0.7129 $\mu A\ \mu M^{-1}$, respectively, representing improved sensitivity over ionic liquid OPPF[15] or CNT modified carbon plate electrodes and other modification methods of various electrode types, as summarized in Table II, suggesting that the developed CPAN5G-4x electrode is also highly sensitive to DA.

Determination of DA in Human Serum

To evaluate the performance of the CPAN5G-4x electrode, which can be used to detect DA in complex biological media, the same measurements were successfully performed in human serum. Known concentrations of DA (0.5–100 μM) were dissolved in serum. Subsequently, the protein in the serum was precipitated by TCA and centrifugation. The serum supernatants were used for further SWV analysis. The calibration curves for

Table II. Comparison of the Proposed Electrode to Other Modified Electrodes for DA Detection

No	Modification of electrode		Sensitivity ($\mu A\ \mu M^{-1}$)	Linear range (μM)	Detection limit (μM)	Reference
	Electrode type	Modification method				
1	Glassy carbon	SDS/Modified graphene oxide	0.066	1-15	0.27	18
2	Glassy carbon	SDS/CNT	0.024	20-200	-	43
3	SPCE	Ionic liquid OPPF	0.026	1-25	0.50	15
4	SPCE	Enzyme/β-cyclodextrin/CNT	0.030	10-50	0.48	17
5	SPCE	SDS/paper-based	0.187	1-100	0.37	10
6	SPCE	SDS/carbonized PAN loaded G fiber	0.721	0.5-100	0.07	This work

Abbreviations: G: graphene; PEDOT: poly(3,4-ethylenedioxythiophene); CTAB: cetyltrimethyl ammonium bromide; SDS: Sodium dodecyl sulfate; CNT: carbon nanotube; SPCE: screen-printed carbon electrode; Au: gold; OPPF: n-octylpyridinum hexafluorophosphate.

DA in human serum were linear in the range of 0.5–100 μM, with a correlation coefficient of 0.9929 ($n = 3$). Recovery experiments were performed by the standard addition method by spiking 10, 20, and 40 μM into the serum samples. The recovery ranged from 104.7 to 110.9%, and the RSD ($n = 3$) was below 3.0% as shown in Supporting Information, suggesting that DA can be selectively, sensitively, and accurately detected at CPAN5G-4x electrodes in human serum in the presence of SDS.

CONCLUSIONS

A carbonized composite nanofiber containing G particles was successfully prepared by electrospinning and carbonization processes. A modification method involving drop-casting CPAN5G-4x suspended in water onto an SPCE WE resulted in enhanced electrochemical activity toward the ferri/ferrocyanide redox couple and DA, as measured using CV and SWV, respectively. The carbonized nanofiber/G composite enabled excellent electron transfer between the DA molecules and electrode surface in the presence of SDS and interferents (AA and UA). This modified electrode was able to determine the presence and quantity of DA in human serum with higher sensitivity and a lower LOD than several previous surface modifications, as summarized in Table II. This simple modification method can likely be used for the fabrication of other high-performance biosensors.

ACKNOWLEDGMENTS

This work was supported in part by the Chulalongkorn University Dutsadi Phiphat Scholarship and Prof. Orawan Chailapakul, Electrochemistry and optical spectroscopy research unit, Faculty of Science, Chulalongkorn University, Thailand. The authors are thankful to Prof. Schwank's research group, University of Michigan, USA for the use of muffle oven.

REFERENCES

1. Sauerbier, A.; Ray Chaudhuri, K. *Basal Ganglia* **2013**, *3*, 159.
2. Zhang, J.; Zhu, L.; Du, J.; Liu, B. *Neural Regen. Res.* **2007**, *2*, 18.
3. Liu, L.; Li, Q.; Li, N.; Ling, J.; Liu, R.; Wang, Y.; Sun, L.; Chen, X. H.; Bi, K. *J. Sep. Sci.* **2011**, *34*, 1198.
4. Heinz, A.; Przuntek, H.; Winterer, G.; Pietzcker, A. *Nervenarzt* **1995**, *66*, 662.
5. Venton, B. J.; Wightman, R. M. *Anal. Chem.* **2003**, *75*, 414 A.
6. Song, P.; Mabrouk, O. S.; Hershey, N. D.; Kennedy, R. T. *Anal. Chem.* **2012**, *84*, 412.
7. Wallenborg, S. R.; Nyholm, L.; Lunte, C. E. *Anal. Chem.* **1999**, *71*, 544.
8. Huang, H.; Gao, Y.; Shi, F.; Wang, G.; Shah, S. M.; Su, X. *Analyst* **2012**, *137*, 1481.
9. Kumbhat, S.; Shankaran, D. R.; Kim, S. J.; Gobi, K. V.; Joshi, V.; Miura, N. *Biosens. Bioelectron.* **2007**, *23*, 421.
10. Rattanarat, P.; Dungchai, W.; Siangproh, W.; Chailapakul, O.; Henry, C. S. *Anal. Chim. Acta* **2012**, *744*, 1.
11. Wightman, R. M. *Science* **2006**, *311*, 1570.
12. Atta, N. F.; Galal, A.; El-Ads, E. H. *Electrochim. Acta* **2012**, *69*, 102.
13. Huang, Q.; Zhang, H.; Hu, S.; Li, F.; Weng, W.; Chen, J.; Wang, Q.; He, Y.; Zhang, W.; Bao, X. *Biosens. Bioelectron.* **2014**, *52*, 277.
14. Zhao, J.; Yu, Y.; Weng, B.; Zhang, W.; Harris, A. T.; Minett, A. I.; Yue, Z.; Huang, X.-F.; Chen, J. *Electrochem. Commun.* **2013**, *37*, 32.
15. Ping, J.; Wu, J.; Ying, Y. *Electrochem. Commun.* **2010**, *12*, 1738.
16. Ku, S.; Palanisamy, S.; Chen, S.-M. *J. Colloid Interface Sci.* **2013**, *411*, 182.
17. Alarcón-Ángeles, G.; Guix, M.; Silva, W. C.; Ramírez-Silva, M. T.; Palomar-Pardavé, M.; Romero-Romo, M.; Merkoçi, A. *Biosens. Bioelectron.* **2010**, *26*, 1768.
18. Zhu, W.; Chen, T.; Ma, X.; Ma, H.; Chen, S. *Colloids Surf. B* **2013**, *111*, 321.
19. Alwarappan, S.; Erdem, A.; Liu, C.; Li, C. Z. *J. Phys. Chem. C* **2009**, *113*, 8853.
20. Nataraj, S. K.; Yang, K. S.; Aminabhavi, T. M. *Prog. Polym. Sci.* **2012**, *37*, 487.
21. Patil, S. A.; Chigome, S.; Hägerhäll, C.; Torto, N.; Gorton, L. *Bioresour. Technol.* **2013**, *132*, 121.
22. Mo, J. W.; Ogorevc, B. *Anal. Chem.* **2001**, *73*, 1196.
23. Zheng, J.; Zhou, X. *Bioelectrochemistry* **2007**, *70*, 408.
24. Tong, Y.; Li, Z.; Lu, X.; Yang, L.; Sun, W.; Nie, G.; Wang, Z.; Wang, C. *Electrochim. Acta* **2013**, *95*, 12.

25. Shahrokhian, S.; Zare-Mehrjardi, H. R. *Sens. Actuators B* **2007**, *121*, 530.
26. Kampalanonwat, P.; Supaphol, P. *ACS Appl. Mater. Interfaces* **2010**, *2*, 3619.
27. Aykut, Y.; Pourdeyhimi, B.; Khan, S. A. *J. Appl. Polym. Sci.* **2013**, *130*, 3726.
28. Das, S.; Wajid, A. S.; Bhattacharia, S. K.; Wilting, M. D.; Rivero, I. V.; Green, M. J. *J. Appl. Polym. Sci.* **2013**, *128*, 4040.
29. Ekabutr, P.; Chailapakul, O.; Supaphol, P. *J. Appl. Polym. Sci.* **2013**, *130*, 3885.
30. Diouri, N.; Baitoul, M.; Maaza, M. *Nanomaterials* **2013**, 2013.
31. Karacan, İ.; Erdoğan, G. *Polym. Eng. Sci.* **2012**, *52*, 937.
32. Saha, B.; Schatz, G. C. *J. Phys. Chem. B* **2012**, *116*, 4684.
33. Liu, B.; Lian, H. T.; Yin, J. F.; Sun, X. Y. *Electrochim. Acta* **2012**, *75*, 108.
34. Huang, Y.-L.; Baji, A.; Tien, H.-W.; Yang, Y.-K.; Yang, S.-Y.; Wu, S.-Y.; Ma, C.-C. M.; Liu, H.-Y.; Mai, Y.-W.; Wang, N.-H. *Carbon* **2012**, *50*, 3473.
35. Gu, S.-y.; Wu, Q.-l.; Ren, J. *New Carbon Mater.* **2008**, *23*, 171.
36. Molnár, K.; Vas, L. M. Electrospun composite nanofibers and polymer composites. In Synthetic Polymer–Polymer Composites; Bhattacharyya, D., Fakirov, S., Eds.; Hanser, **2012**.
37. Chae, W. C.; Young-Gwang, K.; Oh, H. K.; Inn-Kyu, K. *Carbon Lett.* **2007**, *8*, 313.
38. Njagi, J.; Andreescu, S. *Biosens. Bioelectron.* **2007**, *23*, 168.
39. Atta, N. F.; Galal, A.; Ahmed, R. A. *Bioelectrochemistry* **2011**, *80*, 132.
40. Chauhan, N.; Narang, J.; Pundir, C. S. *Analyst* **2011**, *136*, 1938.
41. Rodthongkum, N.; Ruecha, N.; Rangkupan, R.; Vachet, R. W.; Chailapakul, O. *Anal. Chim. Acta* **2013**, *804*, 84.
42. Hou, S.; Kasner, M. L.; Su, S.; Patel, K.; Cuellari, R. *J. Phys. Chem. C* **2010**, *114*, 14915.
43. Zheng, D.; Ye, J.; Zhang, W. *Electroanalysis* **2008**, *20*, 1811.